National Science Foundation (NSF) CMS 01-96120:
Development of Modular Connections for Seismic Resistant Steel Moment Frames
Interim Progress Report to AISC: August 25, 2002

Scope of the Report

This report summarizes the steel connection research performed at the University of Arizona during the spring and summer of 2002. This work is a continuation of NSF-funded research on the development of new seismic-resistant steel connection forms initiated at the University of Notre Dame. The research has been supported by industry partners, most notably the American Institute of Steel Construction (AISC) and the Steel Founders Society of America (SFSA).

Since arriving at the University of Arizona in August 2000, the research team has: (1) designed, fabricated and erected a reaction frame for full-scale subassemblage testing; (2) configured and purchased the data acquisition system, instrumentation and loading equipment necessary to perform the full-scale experiments; and, (3) selected and ordered the necessary computer hardware and software to integrate nonlinear finite element analyses with the experimental research. The integrated computation and experimentation laboratory (ICEL) has been operational since October 2001. A schematic and photo of the ICEL reaction frame are shown in Figures 1a,b.

With the ICEL laboratory in place, the research team: (1) developed the new connection concepts into prototypes through the analytical research; (2) identified and worked with industry partners in the casting industry (SFSA member Varicast, Inc. of Portland OR) and the steel construction industry (AISC member Able Steel, Inc. of Mesa AZ) to create the prototypes and fabricate the test specimens; and (3) successfully tested two of the concepts, the panel zone modular node (PZ-MN) and the modular connector (MC) using the FEMA-350 protocols for qualifying seismic details. This report contains a description of the final version of these two prototypes and a description of the experimental program and test results.

Summary

New modular connections are being developed for use in seismic-resistant steel moment frames. The connections are engineered to meet performance requirements corresponding to optimal seismic response. Traditional rolled shapes, configured for use as main structural members, may not necessarily provide the features needed for the connection regions. Therefore, the designs rely on the versatility afforded by the casting process to create connections specifically configured for seismic performance. The designs also rely on advancements in casting technology to ensure that the connections possess the required strength, ductility, and the inherent material isotropy. The impetus for developing the modular connections is the recently discovered susceptibility to fracture of welded connections in steel special moment frames (SMFs) during strong earthquakes. These structures rely on the strength, stiffness and ductility of welded moment connections at the beam-to-column joints to create an efficient lateral-load resisting system (Popov et al, 1989). However, more than 100 SMFs suffered fracture at these welded joints during the Northridge (FEMA-355E, 2000) and Kobe earthquakes (Watanabe et al, 1998). The performance of the welded moment connections has raised questions regarding the reliable ductility of the SMFs. The consensus from research on steel moment connections is that an effective earthquake-resistant connection design should be based on a combination of weld fracture mitigation measures and changes of connection configuration aimed at reducing the stress levels or redirecting the stress flow in the connection (Stojadinovic and Goel, 2000). The concepts shown here attempt to address these recommendations through new modular connection forms.

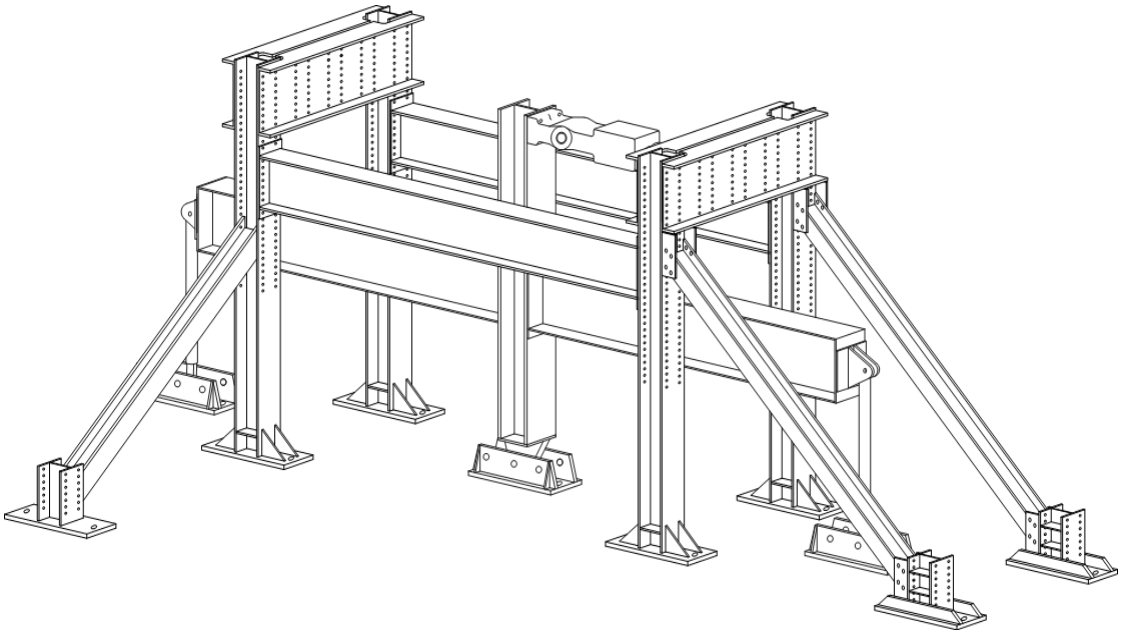

Figure 1. (a): Design schematic of ICEL test frame with subas-

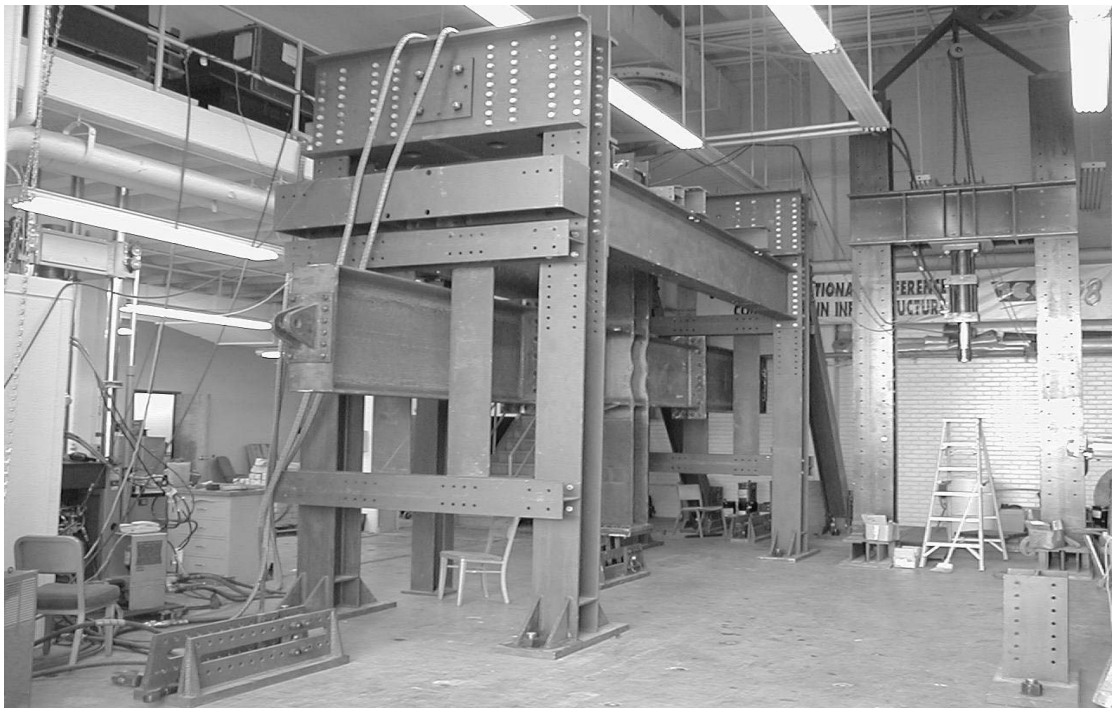

Figure 1. (b): Photo of actual test frame with subassemblage prior to test-

To date, three connection concepts have been developed: (1) a Modular Node (MN); (2) a Modular Connector (MC); and (3) a Post-Tensioned Connecting System (PTCS). This report will focus on the MN and MC concepts tested in 2002. These connections exhibited superior ductility, reliability and energy dissipation characteristics in comparison to traditional connections.

Part I:
Modular Nodes for Steel Special Moment Frames (SMFs)

The modular nodes are created from high-strength high-value steel using a casting process. The major benefit of this approach is the removal of the field weld from the critical beam cross-section at the column face. This represents a significant improvement over traditional construction. In traditional welded-flange connections, the field weld acts as a potential source of brittle fracture (FEMA 350, 2000): First, it is difficult to control the quality of weld and thus flaws may act as the initiation of crack. Second, a heat affected zone (HAZ) develops in which the careful properties of the original parent material may be compromised. Third, the weld requires an access hole in the beam web which creates strain concentrations in the beam. Fourth, the weld location is at a region of high triaxial restraint which could suppress ductile yielding modes in favor of brittle fracture. Finally, the high forces act in the through-thickness (weaker) direction of the column flange. Thus, by removing the weld from critical region the modular node design can greatly reduce the risk of brittle fracture. A field weld does exist farther from the column face at the node/beam interface, a cross-section at which the stresses have been evaluated and minimized.

Two modular node prototypes have been developed: (1) a plastic hinge dissipator (PH-MN); and, (2) a panel zone dissipator (PZ-MN). In each case, the modular node is a cast piece that is shop welded to the column. While the casting approach renders the modular node viable from a manufacturing standpoint, constructability issues must be addressed. Two-tier construction is envisioned in which column assemblages containing two modular nodes are erected; beams are subsequently field-welded to the modular nodes. The modular nodes are intended for use with a range of W14 columns (W14x90 to W14x500) possessing the same inner (T) dimension. It is envisioned that the modular nodes will be available in a limited set of beam depths (W18 to W36).

The PH-MN is still under development and is briefly commented on here. The intent of the PH-MN is to provide a stable and ductile beam plastic hinge region near the column face without the presence of the potentially brittle field weld region at the beam-column flange interface. The PH-MN has features to form a controlled plastic hinge region within the node, reduce flange shear and reduce triaxiality (See Figure 2). Work on the development of the PH-MN continues. A beta prototype is expected by January 2003, and full-scale experimental verification is scheduled for spring 2003.

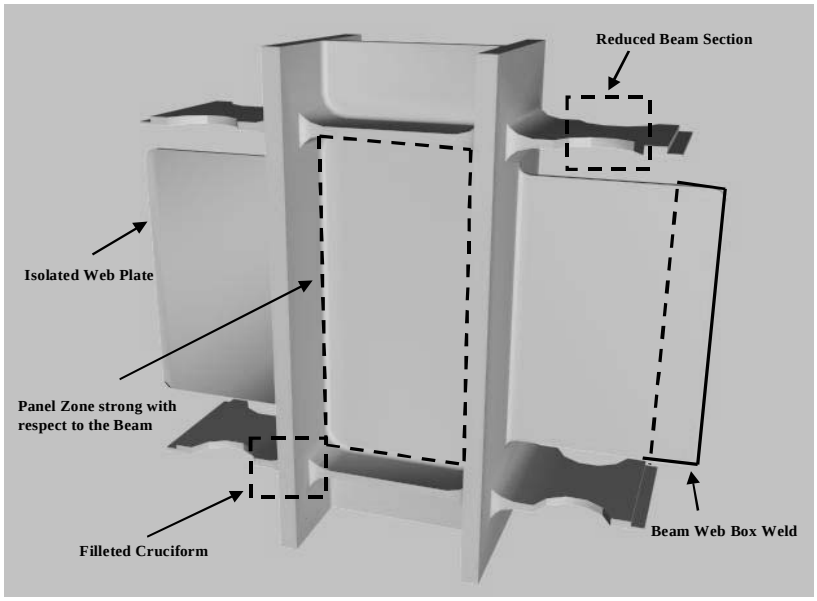

Figure 2. Modular Node trial design (PH-MN).

The PZ-MN prototype has been fully developed and is the focus of Part 1 of this report. A comprehensive analytical investigation of trial configurations and key parameters of the PZ-MN resulted in the selection of a final design. Full-scale prototypes have been created and excellent performance has been shown through full-scale experimentation.

1.A Panel Zone Dissipator Modular Node (PZ-MN)

Under lateral loading of a frame, large shear forces develop in the panel zone due to the action of the opposing moments at the joint (See Fig 3). The design intent of the PZ-MN is to provide the majority of seismic energy dissipation through stable yielding of the panel zone. This region has long been recognized as a stable energy dissipation source for SMFs (Bertero et al. 1972; Krawinkler 1978). However, significant panel zone plastic deformation can be detrimental to connection performance because local curvature ("kinking") of the column flange at the interface with the beam flange produces a high fracture potential at the weld location (El-Tawil, 2000). For this reason, codes have favored developing the ductility of SMFs through the formation of beam plastic hinges (SEAOC, 1996), though limited panel zone plastic deformation is permitted to lower ductility demand on the plastic hinge zone (Popov et al, 1989). Accordingly, the Seismic Provisions for Structural Steel Buildings (AISC, 1997) provides limits to assure proper relative strength of the panel zone to the beam. The SAC Steel Project suggests a balanced approach (FEMA-335D, 2000) in which panel zone and beam yielding initiate simultaneously.

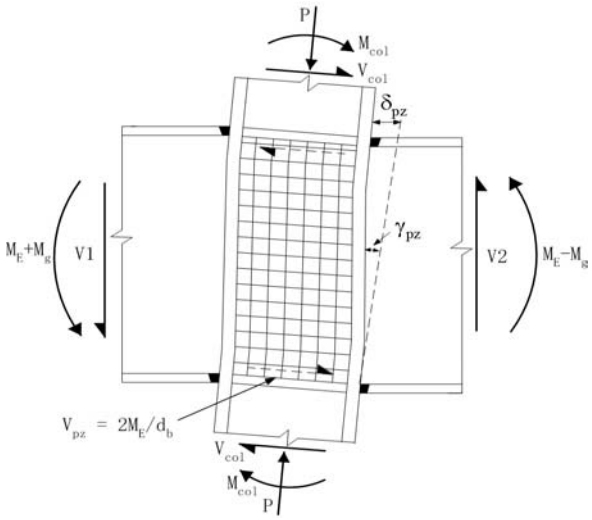

Figure 3. Panel zone deformation.

In contrast, the PZ-MN (See Figure 4) employs a weak panel zone relative to other components (the beam, column, and outer connection region). To accomplish this design, column kinking must be mitigated in order to obviate a high potential for brittle fracture.

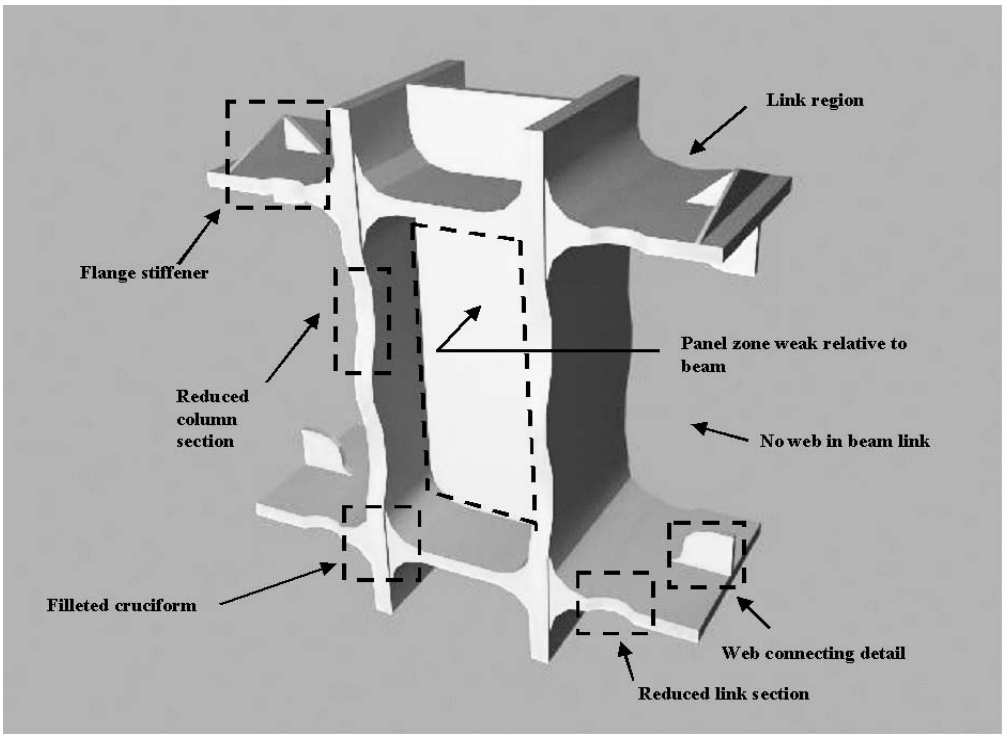

Figure 4. Panel zone dissipator (PZ-MN) configuration.

As indicated in Figure 4, the following features are included in PZ-MN design to achieve this objective: (1) A filleted cruciform to reduce the column flange kinking; (2) The absence of a web in the beam link region to prevent high end shears from developing thereby significantly lowering beam flange bending and plastic strain gradient at the flange/web juncture; (3) Reduced beam and column flange sections in the node to allow controlled yielding outside the panel zone thereby forming a ductile mechanism that minimizes demands at the node/beam interface; (4) Flange stiffeners and a web connection detail that reduce secondary bending at the field weld location and stabilize the beam link flange, respectively. These features were chosen through a comprehensive development program using nonlinear finite element analysis and solid modeling as described in Section 1.C.

1.B Research Program

1.B.1 Analytical Modeling

Two-dimensional (2D) and three-dimensional (3D) finite element (FE) models were used in the development of the modular node. The 2D FE model was used to rapidly evaluate parameters and develop the basic form of the prototype. The 3D FE model was used for verification of the 2D results, experimental predictions, and torsional stability examinations. Models transition from solid to line elements and include material nonlinearity and large deformation. The 3D FE model is shown in Figure 5.

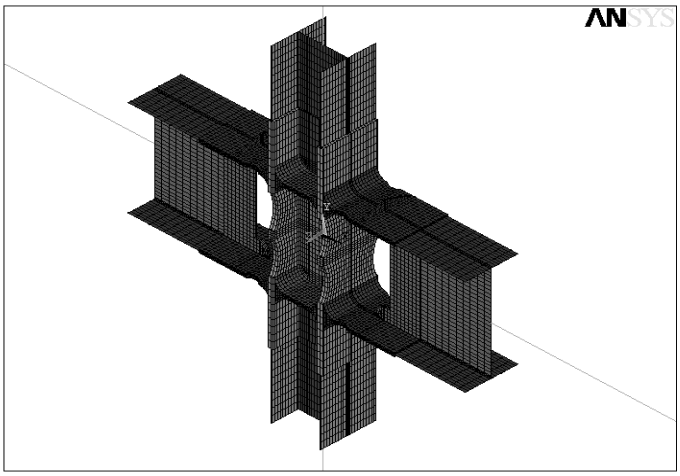

Figure 5. 3D FE model of PZ-MN subassemblage.

1.B.2 Full-scale experimentation

Four full-size PZ-MN prototypes were created by Varicast, Inc. Quality control of the casting process was employed to ensure the PZ-MN prototype possessed the expected ductility. The material for the prototype is mild steel, normalized and stress relieved through heat treatment (See Table 1).

Table 1:

Name	F_y (ksi)	F_u (ksi)	Elongation (%)
PZ-MN	43	67.6	32

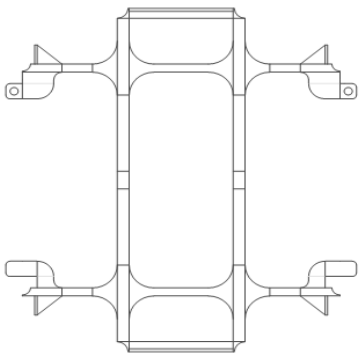

Figure 6a. PZ-MN prototype shop drawing

A shop drawing for the PZ-MN prototype is shown in Figure 6a. Figure 6b shows the PZ-MN prototype at the foundry following removal of the sand molds. The test subassemblages were fabricated by AISC member Able Steel Fabricators, Inc. (Mesa, Arizona) using W14x193 col-

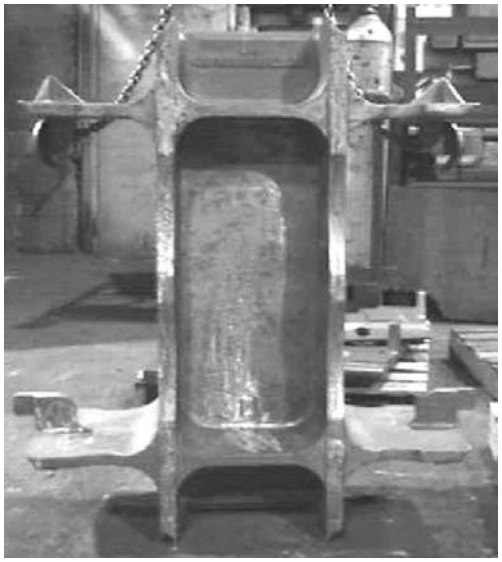

Figure 6b. PZ dissipator.

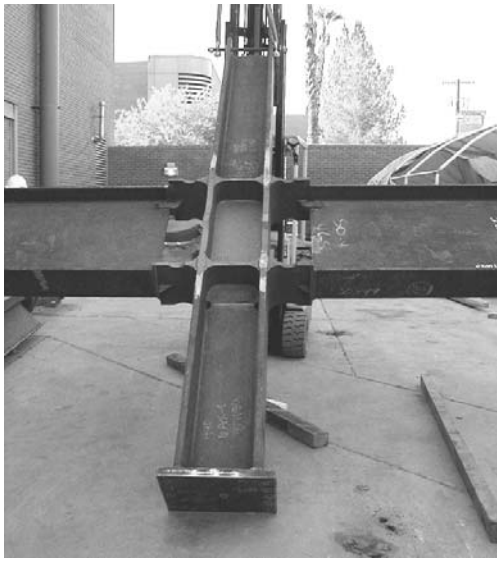

Figure 6c. PZ dissipator subassem-

umns and W30x99 beams. Figure 6c shows the fabricated PZ-MN assemblage being erected at the University of Arizona ICEL laboratory.

.Sufficient lengths of W30 beams were not readily available, and since the outer beam regions remain elastic during the experiments, Able Steel fabricated reusable outer beam fixtures to connect to the inner (test) beam by end-plate splices (See Figure 7). The inset shows the assemblage in place in the ICEL reaction frame.

Figure 7. Test subassemblage with reusable outer beams fixtures. **Inset:** Photograph of subassemblage inside the ICEL reaction frame.

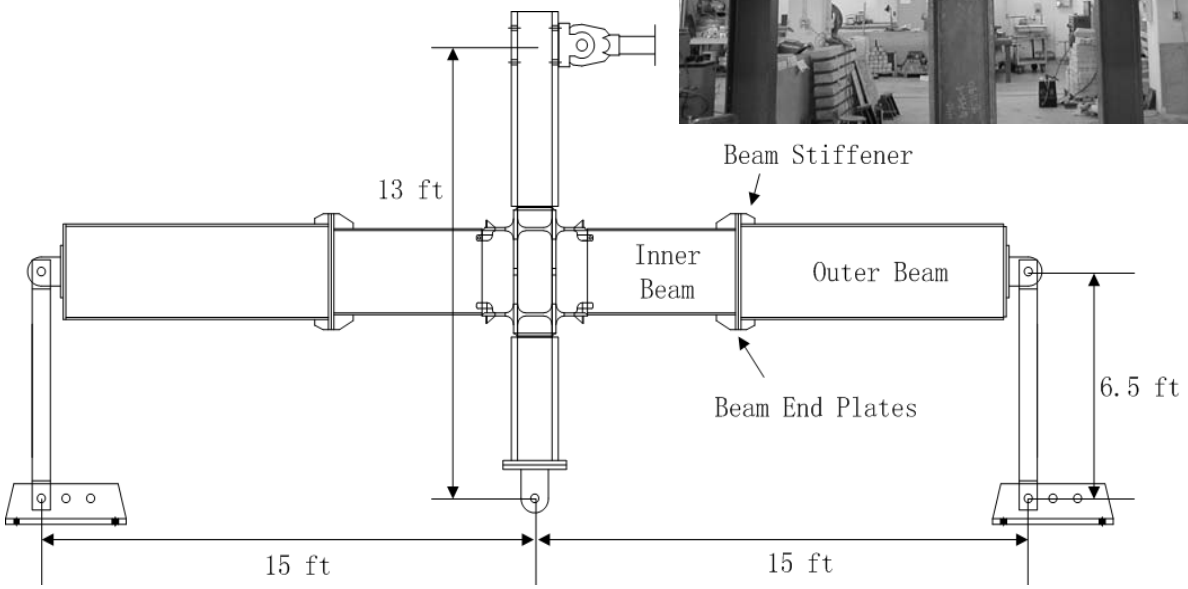

1.C Development of PZ-MN Concept

Each feature indicated in Figure 4 was selected or optimized through the analytical modeling. Filleted cruciforms that minimize kinking (See Section 1.C.1.), in conjunction with measures to ensure a full joint mechanism (See Sec. 1.C.2) and the elimination of local flange bending (See Sec. 1.C.3) create an extremely efficient and ductile energy dissipating detail.

1.C.1 Stable Panel Zone Energy Dissipation

Cruciforms (See Figure 4.) reduce the column flange kinking at the intersection with the beam flange during large panel zone plastic distortion (See Sec. 1.C.1) (The cruciforms also minimize triaxiality, though this action is more crucial for the PH-MN). The elimination of kinking effects allows large plastic shear strains to develop in the panel zone without the potential for fracture at the column face.

Figure 8 shows plots of: (a) the percentage energy dissipated by the panel zone; and (b) the corresponding column flange "kinking" measured as column flange local curvature versus panel zone strength (indicated by $\Omega = M_{p,bm}/V_{y,PZ}$ at 0.05 rad story drift. As expected in the traditional connection, as the panel zone gets weaker (Ω increases), more energy is dissipated but with greater column kinking, i.e. possibility of weld fracture. In contrast, the PZ-MN does not exhibit rapid increases in column flange kinking as more energy is dissipated in the panel zone. For reference, approximate Ω values associated with recent codes are indicated on the plot and give an indication of the column curvature deemed tolerable in design (corresponding to a value of 0.001 rad). It is noticed that (due to the presence of the cruciforms) the PZ-MN can actually be designed to dissipate nearly all of the seismic energy in the panel zone while incurring less column flange "kinking" than occurs in current "balanced" designs, all the time without a weld at the beam-column flange interface. The inclusion of the cruciform in a casting is trivial (actually it improves the integrity of the casting).

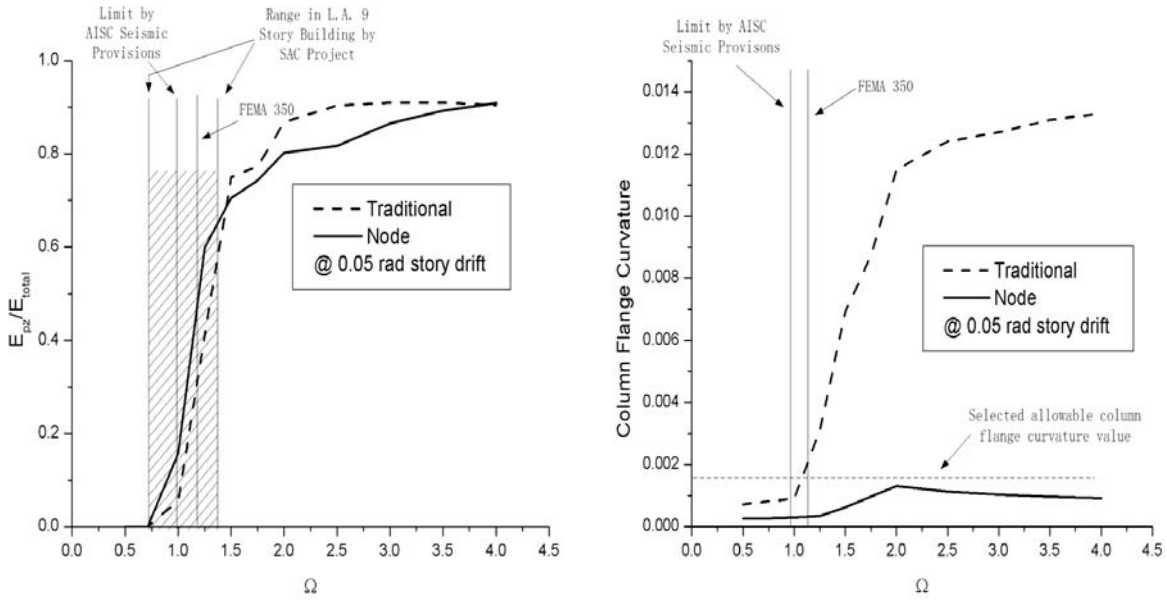

Figure 8. Performance vs. Ω: (a) PZ energy dissipation; (b) Column flange "kinking".

1.C.2 Shear-Induced Interface Strains

The combination of a weak panel zone and *the* cruciforms has been shown to provide stable behavior in the PZ-MN. However, these features are not enough in themselves to produce ductile behavior for the entire joint. The high stiffness provided by the cruciform, effective in preventing kinking, exacerbates the high restraint in the web near the beam-column flange interface. Figure 9, a plot of the equivalent plastic strain of an early version of the PZ-MN (containing a web connection), shows that the maximum strain demand exists at beam-column juncture, rather than within the panel zone. This high strain region compromises the design objective of the PZ-MN.

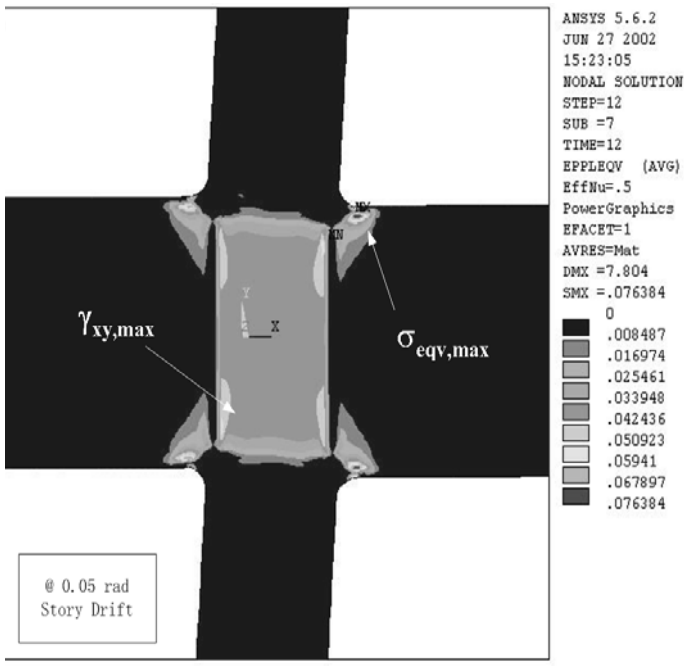

Figure 9. ε_{eqv} distribution for a early PZ-MI

A web in the PZ-MN beam link region was ultimately recognized as detrimental because: (1) it causes beam flange shear and beam web shear higher than total beam shear; and (2) it increases the plastic strain outside the panel zone through high constraint. As the beam link flange itself can sustain the beam shear, a viable solution for the PZ-MN is to eliminate the web in the beam link region and form a beam mechanism (Shown in Figure 10a,b).

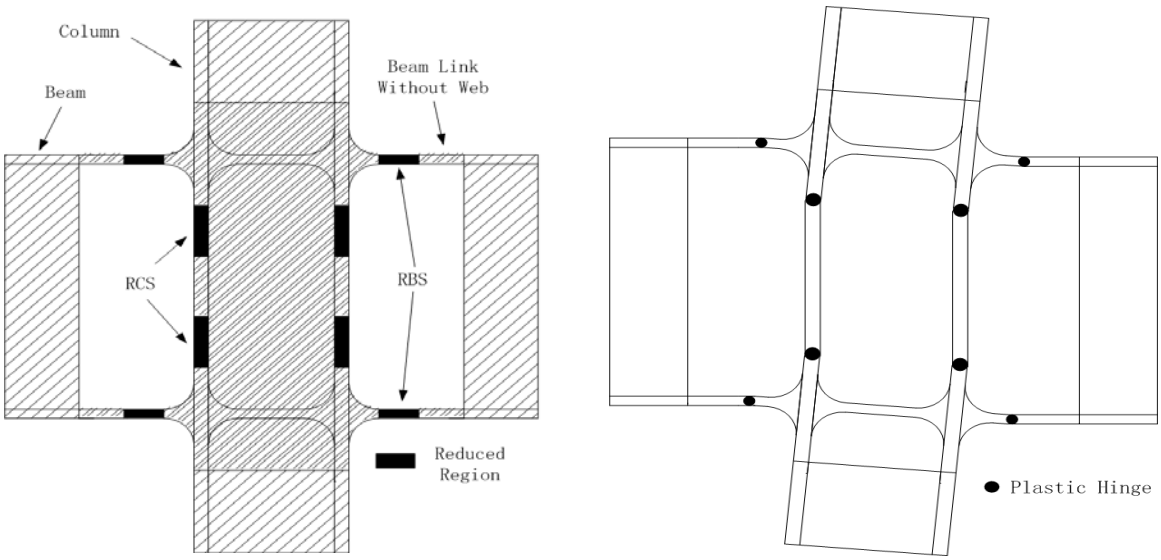

Figure 10. PZ-MN mechanism: (a) location of reduced sections; (b) deformed shape.

1.C.3 Local Flange Bending

Two features were added to the beam link region of the PZ-MN to reduce the stress at the weld and keep the weld elastic at 0.05 rad of story drift. These include: (1) a web connector; and (2) a flange stiffener. The efficacy of these features was verified in the experiments.

I.D. Experimental Verification

Both monotonic and cyclic experiments were scheduled and tested (See Table 2). Table 3 shows the global properties from the experiments and the analytical comparisons. The anticipated full joint mechanism identified in the FE analysis was verified in the experiments (See Fig. 11).

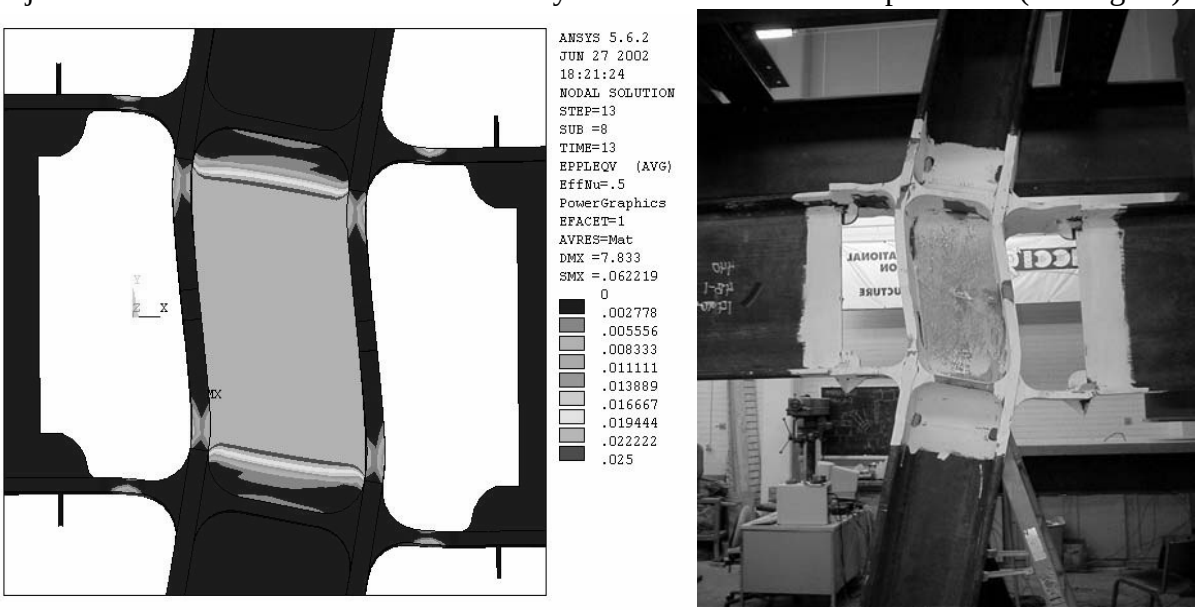

Figure 11. Development of full mechanism: (a) in FE analysis; (b) in full-scale experiment

Table 2: Full Scale Test Descriptions

Name	Test ID	Type of Loading	Column	Inner Beam	Outer Beam	Status
PZ-MN	PZ-MN-1	Monotonic	W14x193	W30x99	W33x118	Completed
	PZ-MN-2	Cyclic (FEMA350)	W14x193	W30x99	W33x118	Completed
	PZ-MN-2	Cyclic (gravity Load)	W14x193	W30x99	W33x118	01/03/2003

Table 3: Summary of the test results

Name	Type	K_i (kip/in)	K_2 (kip/in)	P_y (k)	P_u (k)	Θ_u (rad)
PZ-MN-1 (Monotonic)	FE	95	4.1	76	113	0.05
	Experiment	75	5.9	70	161	0.18
PZ-MN-2 (Cyclic)	FE	95	4.1	76	-	-
	Experiment	69	-	70	181	0.077 (14 cycles)

1.D.1.1 Test PZ-MN-1: Monotonic

Figure 12 shows load vs. tip displacement for Test PZ-MN-1. Also indicated on the figure is the analytical prediction by the 3D-FE subassemblage. The results exhibit excellent agreement.Each load-unload segment indicates the test set-up reaching its stroke capacity and being reset. At the ultimate drift angle (0.18) the PZ-MN and its connections to the main members had not failed and were not in any imminent danger of doing so; it simply made little sense to continue the test further. Figure 12b shows the deformed shape of the specimen at a subassemblage drift of 0.18 rad.

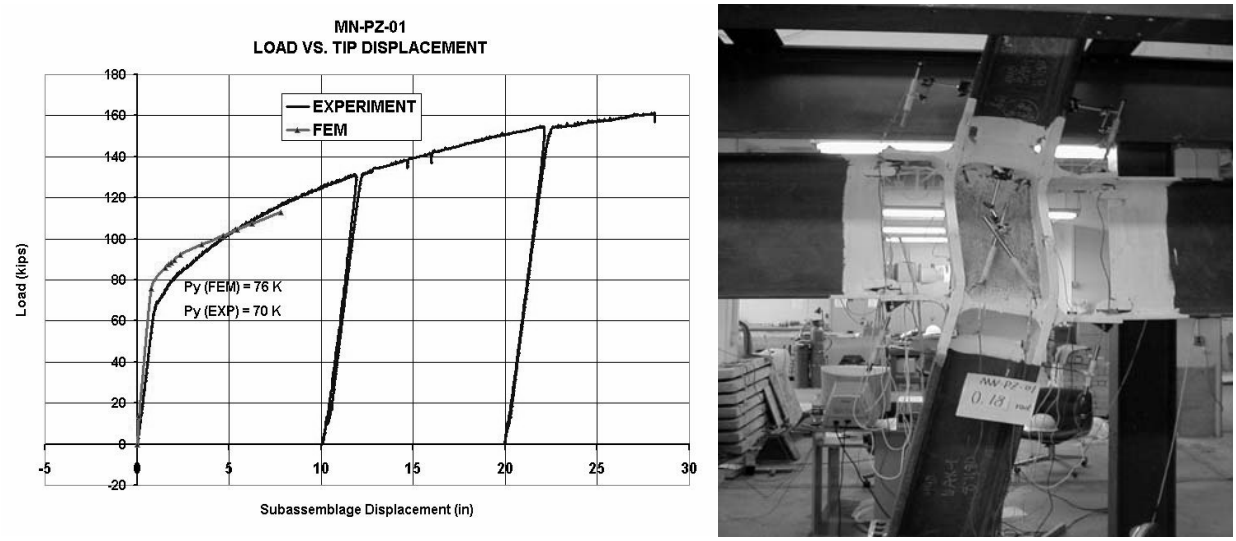

Figure 12. PZ-MN1 Subassemblage Global Response: Load-Deflection.

1.D.1.2 Test PZ-MN-2: Cyclic

Experiment PZ-MN-2 tested the prototype under the FEMA-350 load protocol. Figure 13a shows the global load vs. tip displacement for Test PZ-MN-2. The test results indicate remarkable cyclic performance: The PZMN survived the FEMA 273 protocol with no distress up to the actuator stroke limit (± 0.077 rad). The yellow lines indicate the acceptance drift for new connection designs in high seismic zones. The PZ-MN had no difficulty achieving this value and did not fracture at the maximum drift values shown. Instead, it was cycled an additional 12 times at the maximum displacement before a low-cycle fatigue failure was incurred in the panel zone. Figure 13 shows this ultimate failure of the specimen. It should be noted that neither the shop welds between the node and the column nor the field welds between the node and the beam suffered distress. The strain gage rosettes and LVDTs in the panel zone, link and at the welds verified the analyses (Strain gages indicated it essentially remained elastic as intended). The dotted line in Figure 13 indicates the monotonic envelope. Note that incredible work hardening occurs in cyclic test.

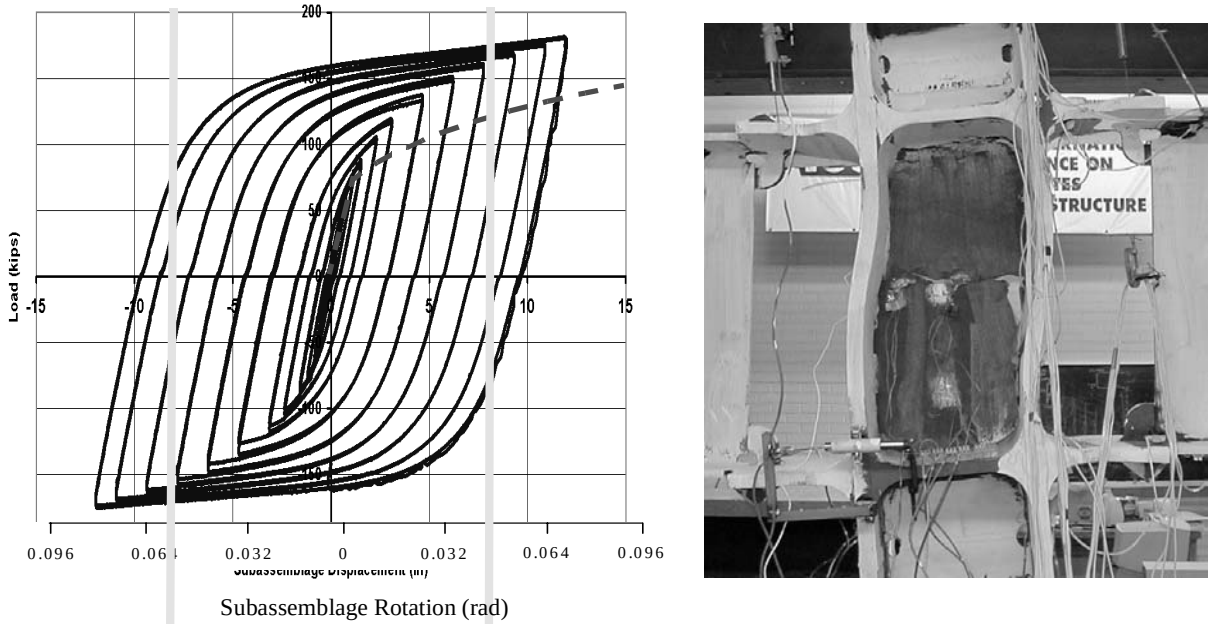

Figure 13. PZ-MN2 Subassemblage Global Response: (a) Load-Deflection (b) picture at failu

Part II
Modular Connectors for Seismic Resistant Steel Moment Frames

The modular connector (MC) is a cast piece used to connect the beam flange to the column. It is envisioned that typical construction will involve shop-welding the MC to beam flanges and field-bolting the MC to the column flange (See Figure 14). The connectors possess a certain level of compliance, thus the joint will be, strictly speaking, semi-rigid. However, high rotational stiffness is achievable, and thus the MC provides a bolted alternative for full-moment connections that eliminates the potential for brittle behavior associated with welding construction. The MC is engineered to deliver reliable and repeatable energy dissipation through improved cyclic ductility. This objective is achieved through the elimination of concentrated plastic strain regions and the reduction in bolt prying forces. The geometry required to produce such outcomes is not necessarily available in the configuration or fastening procedures associated with traditional rolled shapes. Thus, as with the MN, the MC will utilize the versatility afforded by casting processes to obtain optimal geometric configurations.

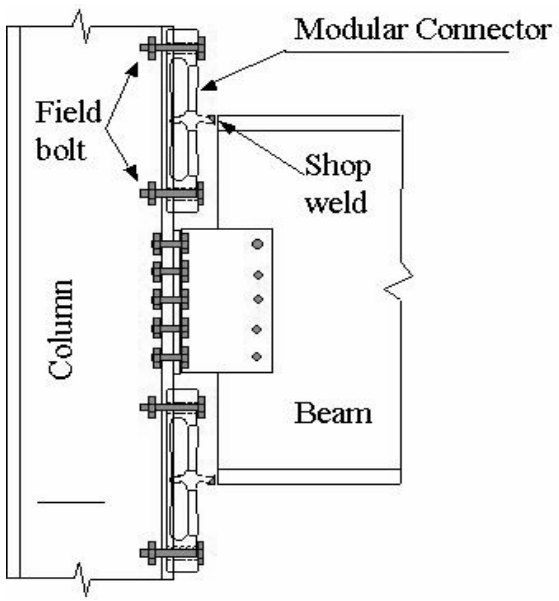

Figure 14. Location of Modular Connector

The MC is similar in form to the WT sections used in the traditional bolted tee-stub connection. However, the MC configuration contains major modifications that distinguish it from the WT (see Figure 15). Foremost among these modifications are: (1) end regions configured to reduce bolt prying forces; and (2) principal flexural spans (arm elements) transitioned into a variable cross-section piece to reduce plastic strain demand. Each of these features is elaborated in the following.

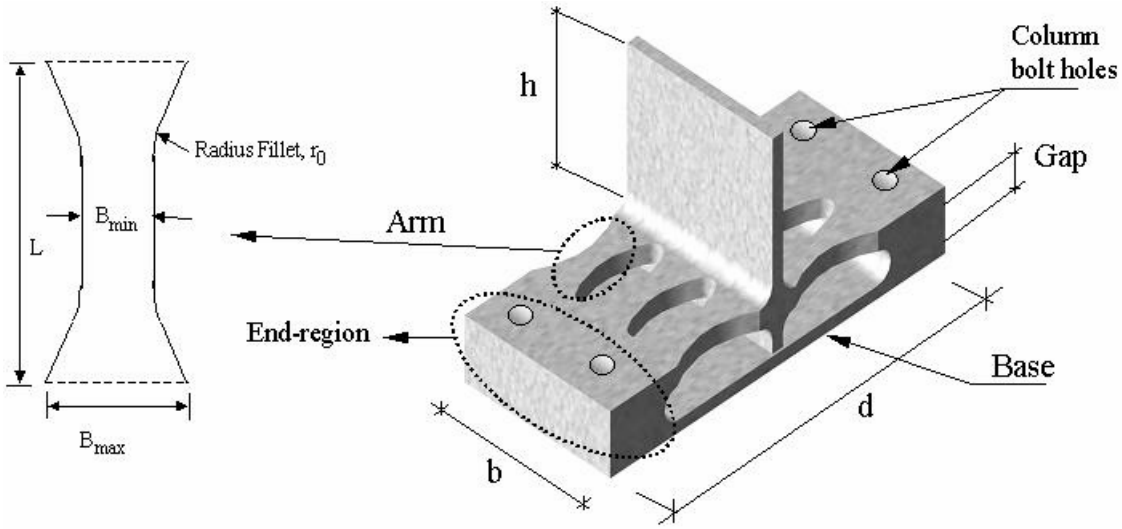

Figure 15. Typical configuration of modular connector.

(1) End-regions: The configuration of the end region is designed to minimize the prying forces that develop in the bolts under tension load. Reduction of force demands on the bolt is desirable from a capacity design standpoint as the bolt is less ductile than the mild steel detail pieces. The particular feature shown in Figure 15, the base configuration, is one of several end region configurations under investigation (See Fig. 16): (I) Base - containing a back piece connecting each end region, thereby significantly reducing prying and additionally provides a near-fixed boundary for arm flexure; (II) NoBase - used as a control to compare the MC directly to a WT; (III) Outrigger - employing an extending bearing pad which increases the leverage of contact thus decreases prying forces, and (IV) Eccentric: containing secondary bolts eccentric to reduce the rotation of the end-region. Each configuration also possesses a compression pad provided to transmit the beam flange compressive loads directly to the column as the MC cycles between tension and compression loading during seismic response. This feature is necessary to reduce pinching of the hysteresis curves and greatly reduces the cyclic strain demand in the connector arm.

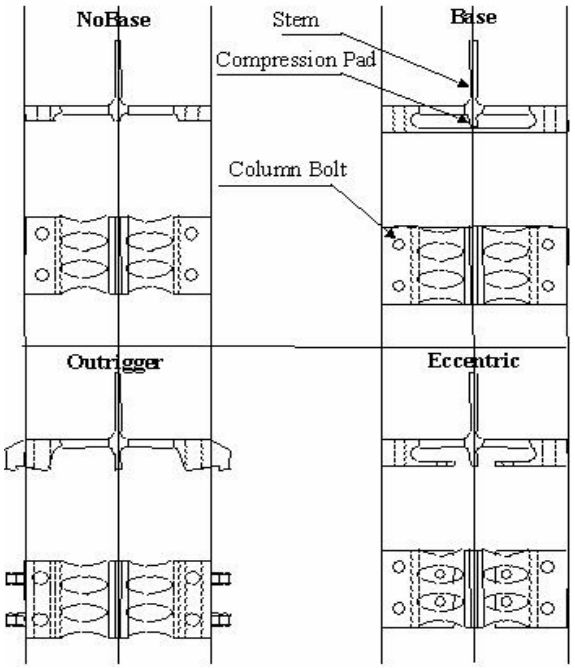

Figure 16. Possible end-region configurations

(2) Arm elements: The intent of the MC design is to develop the ductility within the connector itself. Therefore, the MC is detailed to dissipate energy through plastic deformation in the arm elements. These elements possess variable cross-sections to produce a plastic zone that is distributed along the entire length of the element. Such a distribution will reduce the intensity of strain concentrations that would occur, for instance, with the uniform section of the tee-stub shape. This approach has been used successfully in various metal dampers used primarily for bracing systems, e.g. ADAS devices (Whitaker 1989). However, certain differences exist in this application. Using the region in Figure 17 shown for 3D FE model, to evaluate arm shape, Figure 18a shows three possible configurations: (1) constant width plate as is the case with a WT section; (2) the ADAS geometry (Whitaker, 1989); and (3) the final shape chosen for the MC arm. At high transverse displacement demands, concentration of plastic strain is observed at the ends of the constant width plate as a result of the concentrated plastic hinges

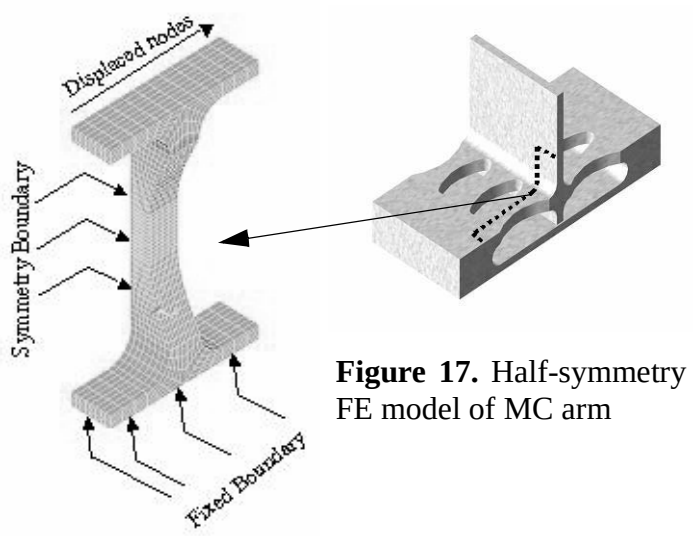

Figure 17. Half-symmetry FE model of MC arm

due to reverse curvature bending. The ADAS geometry obviates this behavior, as has been well documented. However, in this application as a beam-to-column connection, the development of catenary forces causes strain concentration in the middle region. In contrast, a relatively uniform plastic distribution occurs in the MC arm. These geometric ratios were found to be optimum for MCs of practical length through an extensive parametric study. Nevertheless, high strain demand in the center region, analogous to the "necking" of a tensile coupon, will eventually occur. The MC arm is configured such that this behavior occurs beyond ductility demand of interest.

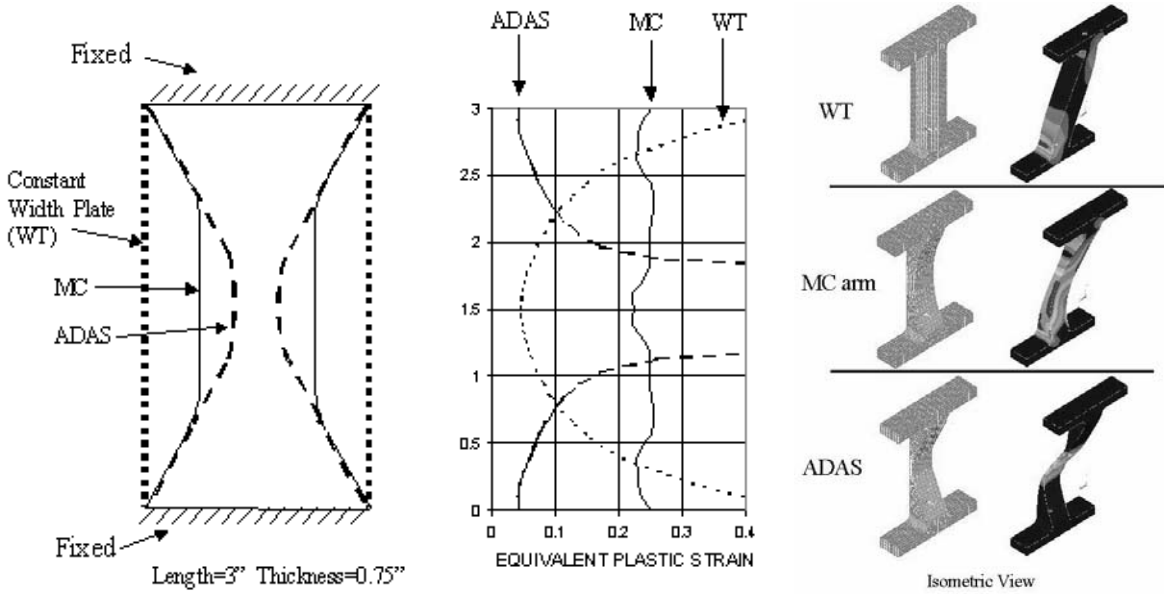

Figure 18a,b. Equivalent plastic strain distribution (0.05rad for 30" beam).

Figure 18c. Distribution of equivalent plastic strain in WT, MC arm and ADAS (0.05rad for 30" beam)

By minimizing the high prying forces and moments that would otherwise occur in bolts, designs with longer gages, i.e. more ductility, can be used. Figure 19 shows FE models of the tee-stub detail piece and the MC of similar strength and stiffness. Equivalent plastic strain is shown in the contours at the identical deformation demand (0.067 rad for a W30 beam).

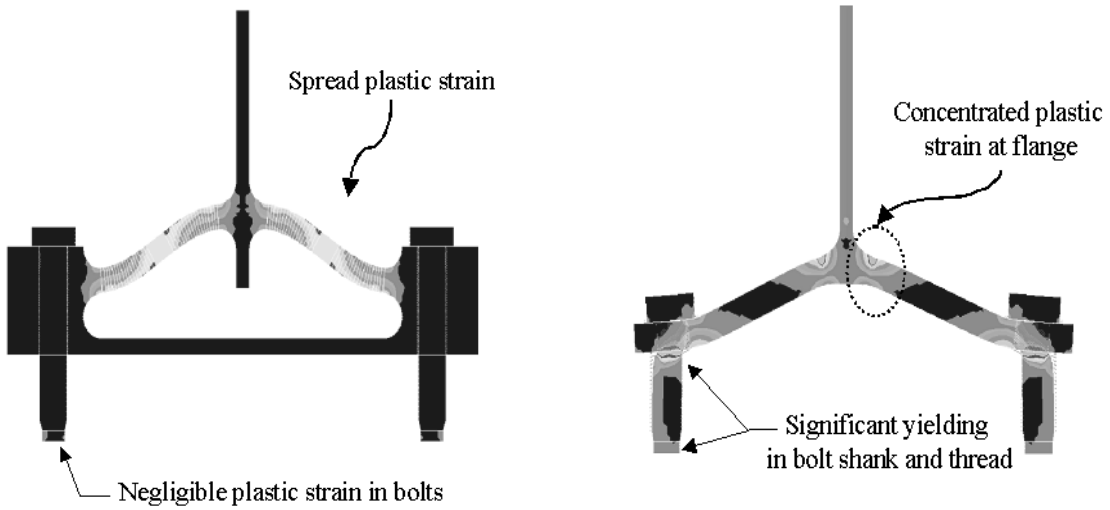

Figure 19. Plastic strains in FE models: (a) MC, (b) tee-stub

2.A Experimental Program

The experimental program consists of two stages: (A) pilot tests of half-scale MCs under direct (beam flange) tension - COMPLETED (B) large-scale subassemblage tests of full-scale MC beam-to-column connections - (Scheduled for early 2003). Material properties and details of the specimens are shown in Appendix A and B.

Pilot Test Program

In the pilot test program, isolated MC and tee-stub specimens of similar strength and stiffness were subjected to direct axial load representing the beam flange force. The pilot tests loading is a simplification of actual conditions where shear forces are also present. However, by testing isolated half-scale MCs (See Figure 20), the MC concept was verified economically and rapidly. This activity primarily involved verifying the reduction in plastic strain demand and bolt prying of the MC prototype configuration indicated in the analytical program.

Figure 20. MC specimen

Figure 22a compares load normalized with yield load versus deflection for monotonic MC and WT tests. The MC achieves an extremely large ductility Δ_u = 2.4 inches corresponding to a θ = 0.1 rad. rotation for a W24 beam. Note that because of the presence of the base, the MC does not incur a bolt failure with a 7/8" A325 bolt while even a 1 1/8" A490 fails with the traditional WT connection. The MC also exhibits greater ductility and overstrength in these monotonic test (Figure 21 shows deformed and undeformed MC). The improvements for cyclic loading are much greater than implied in this graph, as will be shown subsequently. Figure 22b shows one of the failed bolts from the monotonic WT test and equivalent plastic strain contours in the bolt from an analysis of that test. As seen, the anticipated bolt failure mechanism for WT connections observed in the FE analysis was verified by the experiments.

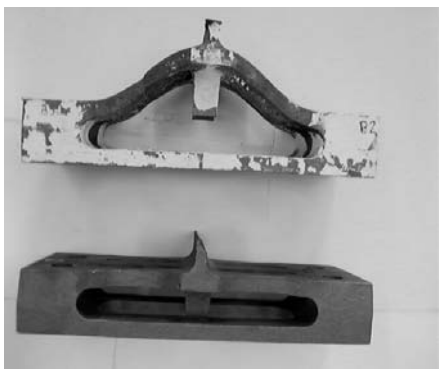

Figure 21. Deformed and undeformed MC

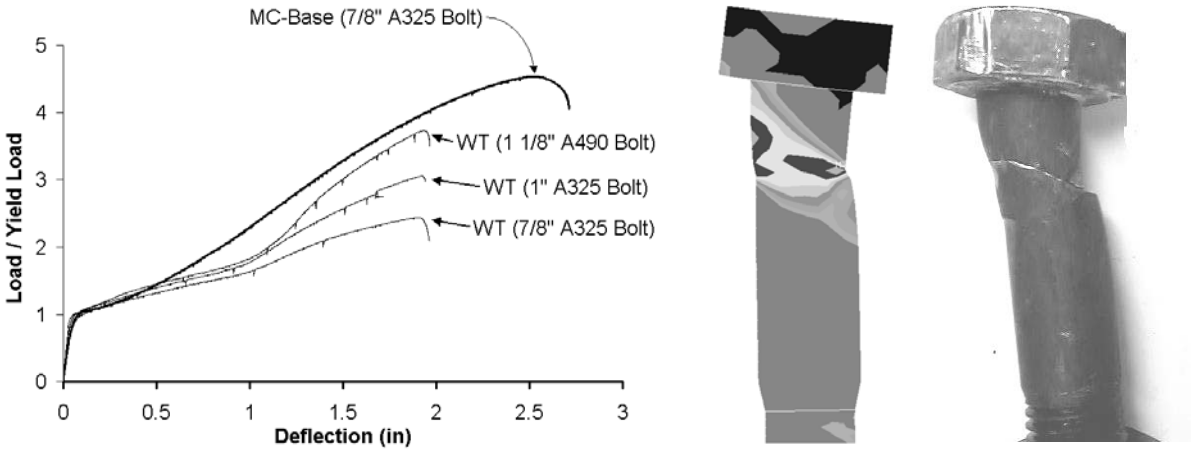

Figure 22. (a) MC and tee-stub comparison: Normalized load vs. deflection; (**b**) Typical Bolt Failure in Tee-Stub Tests: FE and Experiment (1" A325 bolt).

In order to measure axial and flexural strains along the arm, strain gages were applied at five sections (A, B, C, D, and E) along the arm (See Figure 23a). These gages were "Large Strain" with low viscosity epoxy resin strains to measure plastic strains up to 20%. Figure 23b shows a plot of the arm strains at the three specific arm strain regions (A, C, E) versus deflection. It indicates excellent local agreement between the analytical and experimental results. The agreement shown in Figures 23b are typical of all the pilot experiments and thus indicates relatively high assurance that the prototype development decisions based on the extensive analytical program are likely sound.

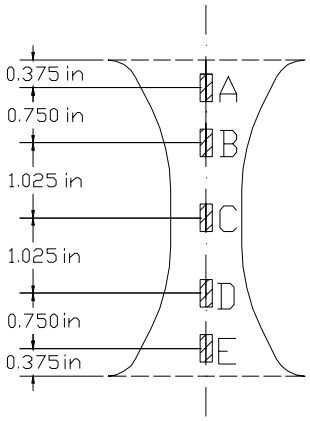

Figure 23a. Strain gage layout on MC arm

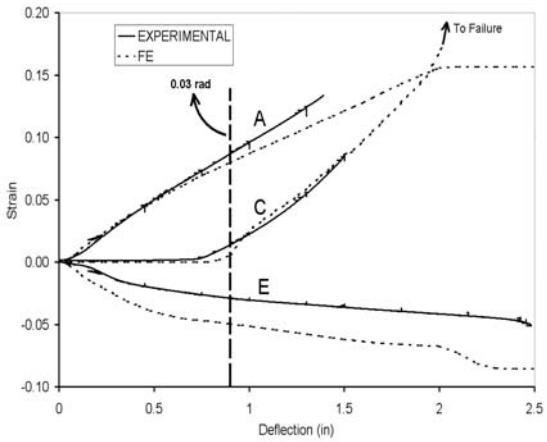

Figure 23b. FE vs. experiment: Strain demand in MC arm.

The failure mode is necking of the center region of the arm (see Figure 24) rather than failure in the high bending regions. It is of importance to note that the development of plastic strain at the critical region is delayed due to the low values of catenary force at lower displacement demands. In fact, the region C (necking region) basically has no plastic strain demand at $\theta < 0.03 rad$ (refer to Fig 23b). What this implies is that the low cycle fatigue life of the MC under significant (0.03 or less) but not extreme cyclic loads may be superior because as indicated in Fig. 23b, the outer (non critical) regions (A,E) will undergo the larger cyclic plasticity while the critical region basically does not incur ductility demand.

This outcome is realized in Figure 25 which shows load versus deflection comparison for constant amplitude test of similar MC and WTs. First it should be noted that just to be able to compare low cycle fatigue life of the WT with the MC, the WT required 1 1/8" A490 bolts while the MC used 7/8" A325. The MC and the tee-stub are cycled at 0.72 inches. After cycling the tee-stub 19 times, the tee-stub failed near the end of the fillet. The MC failed after cycling 44 times. This result was implied by the delayed plastic straining exhibited in Figure 23b.

Figure 24. Close up view of the failure regic

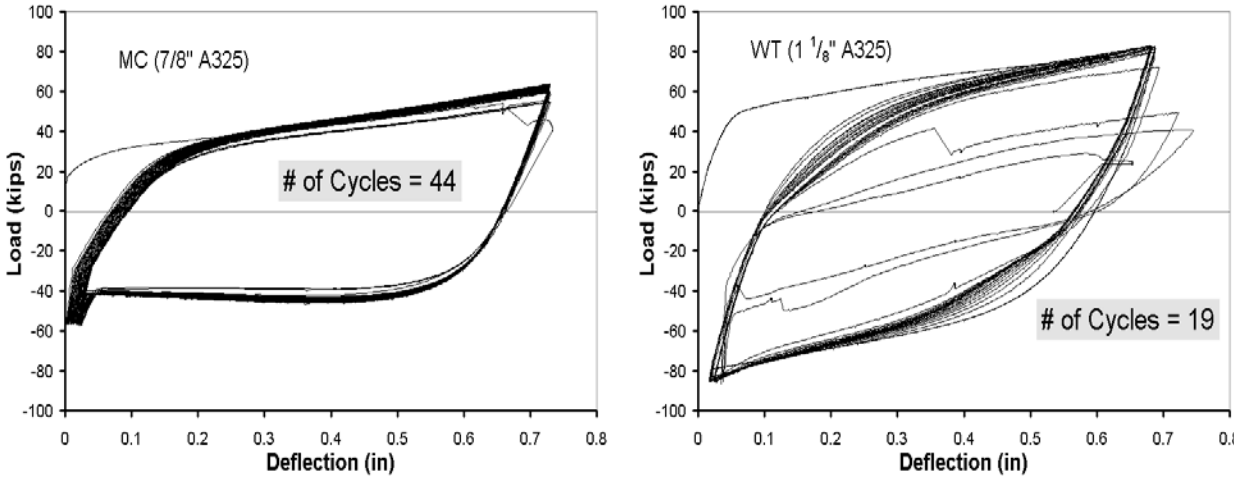

(a) (b)

Figure 25. Load vs. Deflection: (a) MC (b) WT

MC Test Results under FEMA loading protocol

An unforeseen by-product of the catenary action is a twisting instability mode of the MC arms on load (compressive) reversal at very large ductilities. This action slightly reduces the ductility capacity of the MC and causes an alternate failure mode (low cycle fatigue failure at high bending region, most likely A). This behavior and the retrofit that reduces its action such that no ductility reduction exists is described in the following.

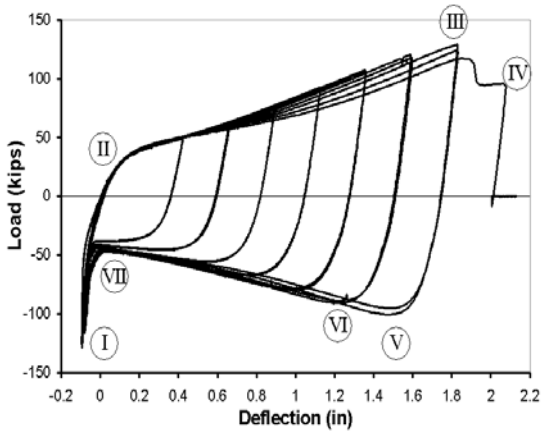

I-Maximum compression
II-Yield Strength
III- Ultimate Strength
IV- Necking Failure at Center of the Arm
V- Unstable Compression Behavior
VI- Stable Compression Behavior
VII- Compression at initial position

Figure 26. MC-Base under cyclic loading

A distinct characteristic of the MC-Base is the widening distance between the positive and negative yield surfaces (See Figure 26 points III and V). This behavior occurs due to the plastic elongation of the arms under catenary forces. On load reversal, the arms are longer than their original dimension. Thus chord action develops in the arms until the load is sufficient to "snap-through" to a "tension-hanger" configuration. These behavior (A) lowers the load required to return the MC back to the column face; and (B) changes the strain increment such that LCF failure can occur at the end regions. The occurrence of the torsional mode has a slight detrimental effect on the global ductility (cyclic and overall) of the MC. For the torsional mode, a plastic hinge is required at the MC stem. Thus, one possible retrofit is to strengthen this region. However, the most promising retrofit which will become a standard feature on the subsequent MC prototype, is to provide the base configuration with guide plates to eliminate the twisting. Figure 27

shows MC with and without guide plates.

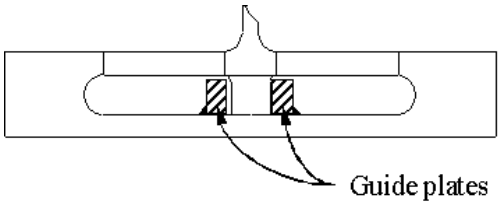

(a)

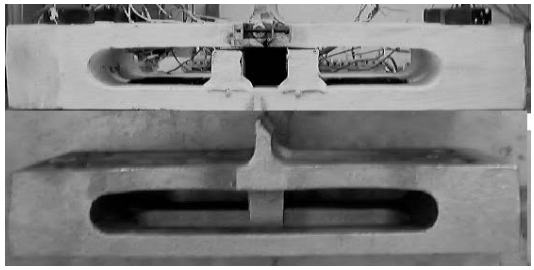

(b)

Figure 27. (a) Location of guide plate, (b) photograph of retrofitted and unretrofitted MC.

MC Tests without the Base under monotonic loading protocol

The MC without Base exhibited superior ductility. At 0.106 radians the necking type failure was observed. Deformed and undeformed shape is shown in Figure 28. Similar to unretrofitted MC cyclic test, test Cyc-NoBase-1 exhibited the twisting instability. The failure occurred at region D.

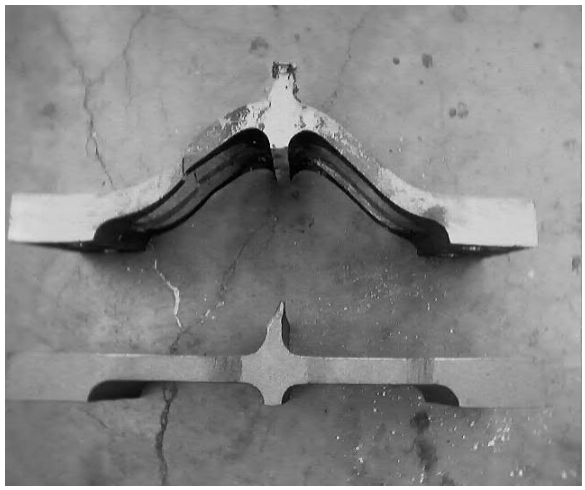

Figure 28. Deformed MC-NoBase under monotonic loading and undeformed MC-No.Base

Conclusions

The cast modular connections have shown great promise as special energy-dissipating details. These modular designs exhibited: (1) Superior ductility with respect to traditional connections; (2) Stable and efficient energy dissipation; (3) Increasing strength; and, (4) Reliability and repeatability.

Appendix A. The mill properties for the MC prototype castings

Table 4: Material properties from mill certification.

Series	F_y (ksi)	F_u (ksi)	Elongation (%)
MC-Base	43	67.6	32
MC-NoBase	48.4	69.4	31.5

Appendix B. Half-scale prototype and WT7x49.5 dimensions

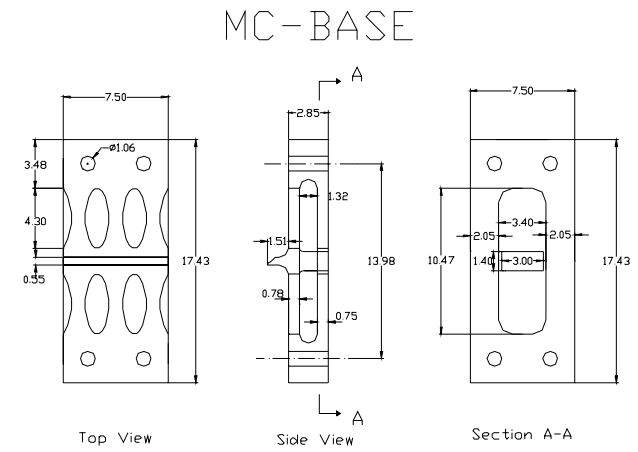

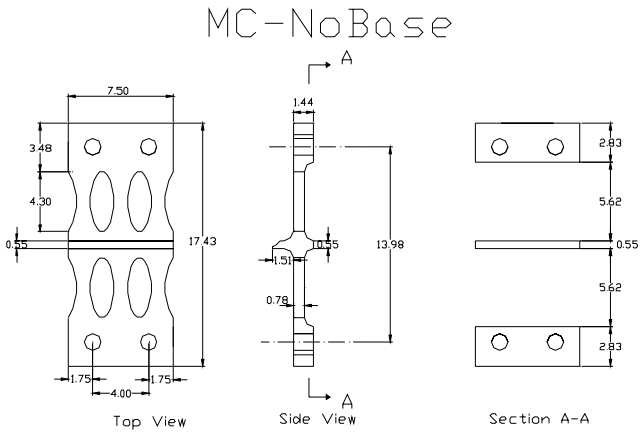

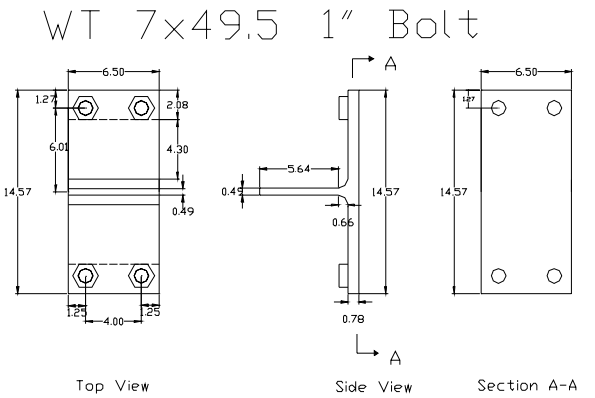

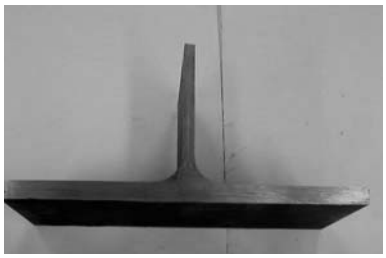

(a) MC-Base, (b) MC-NoBase, (c) WT